Vibrational Spectroscopy 92 (2017) 280–286

Contents lists available at ScienceDirect

Vibrational Spectroscopy

journal homepage: www.elsevier.com/locate/vibspec

Vibrational spectroscopic and density functional study on 1,2,4-triazolo-[1,5-a]pyrimidine

Sibel Çelik[a], Serdar Badoğlu[b,*], Şenay Yurdakul[c]

[a] Ahi Evran University, Health Services Vocational School, Kırşehir, Turkey
[b] University of Turkish Aeronautical Association, Faculty of Air Transportation, Department of Flight Training, Etimesgut, Ankara, Turkey
[c] Gazi University, Faculty of Science, Department of Physics, Teknikokullar, Ankara, Turkey

ARTICLE INFO

Article history:
Received 24 November 2016
Received in revised form 18 August 2017
Accepted 20 August 2017
Available online 25 August 2017

Keywords:
1,2,4-Triazolo-[1,5-a]pyrimidine
Vibrational spectroscopy
DFT
Solvent effects

ABSTRACT

A combined theoretical and experimental investigation on a pharmaceutically important molecule 1,2,4-triazolo-[1,5-a]pyrimidine (TP) is presented in this study. Theoretical Density Functional Theory (DFT) study on the geometry, vibrational properties, energetics, and chemical shifts of the ground state of TP was carried out at B3LYP/6-311++G(d,p) level. Experimental infrared and Raman spectra of TP were presented and complete assignments of all vibrational modes were proposed by using the results of Total Energy Distribution (TED) analysis. The structure, spectra and energetics of TP in chloroform, carbon tetrachloride (CCl_4), methanol, dimethyl sulfoxide (DMSO) and water solvents have been calculated at the same level of theory by employing polarized continuum (PCM) model. Energies, relative stabilities, and dipole moments of TP were also evaluated in the gas phase and in polar and apolar solvents as well.

1. Introduction

1,2,4-Triazolo-[1,5-a]pyrimidine (TP) is a heterocyclic compound which consists of a pyrimidine and a triazole ring fused together. TP, and its derivatives, have been subject to many studies due to its physical and chemical properties [1–3]. They have found applications in pharmaceutical, agricultural and other areas [4–6]. For example, 7-(*N,N*-diethylamine)-5-methyl-1,2,4-triazolo-[1,5-a]pyrimidine is clinically used as a coronary dilator [7] and several 1,2,4-triazolo-[1,5-a]pyrimidine-2-sulfonamides act as active herbicides for the control of broad leaf weeds in cereal crops [8,9]. Several TP derivatives are known as cardiovascular vasodilators [10], dual thrombin/factor Xa inhibitors [11], and human adenosine A_{2a} and A_3 receptor ligands [12–14]. They are also reported to possess potential anti-tumor activities [15–17].

TP derivatives have been the subject of many studies and their physical, chemical, and spectrosopic properties were examined. However, the researches on TPs have been mostly concerned with 5,7-dimethyl-1,2,4-triazolo-[1,5-a]pyrimidine (dmTP) and 4,7-H-5-methyl-7-oxo-1,2,4-triazolo-[1,5a]-pyrimidine (hmTPo). Salas et al. elaborated spectroscopic properties, structural characterization and biological activity of metal complexes of TP and of its several derivatives [18]. Szłyk et al. synthesized several metal complexes of TP derivatives, and investigated them by using X-Ray diffraction and NMR spectroscopy [19–23]. Another study has focused on the synthesis of new TP derivatives, and their use as two-photon absorption spectral properties [24].

Solvent effects play an important role in organic reactivity phenomena such as chemical equilibrium, rate of chemical reactions, conformational preferences, vibrational spectra and biochemical quantities [25]. Solute-solvent interactions (including ion-dipole, dipole-dipole, dipole-induced dipole, and H-bonding interactions) may strongly affect energetic, electronic, and vibrational features of molecular structures [26]. Hence, studying the effects of solvation on chemical entities assists in understanding the possible interactions between any specified molecule and the solvent [27].

The spectroscopic properties of TP have not been studied yet to the best of our knowledge. The importance of this molecule and the lack of information on its molecular properties have been motivated us to investigate geometrical, vibrational, electronic, and energetic features of TP in the gas phase, and in polar and apolar solvents. The most stable ground-state geometry of TP is computed and the results obtained are compared with the data taken from the literature. Experimental FTIR and Raman spectra of TP were recorded, compared with the computation results, and a complete assignment of vibrational bands are proposed depending on the computation results and total energy distribution (TED)

* Corresponding author.
E-mail address: sbadoglu@thk.edu.tr (S. Badoğlu).

http://dx.doi.org/10.1016/j.vibspec.2017.08.011
0924-2031/

analysis. Atomic charges, frontier molecular orbitals, and nuclear magnetic shielding tensors are also obtained theoretically. Besides, geometric and vibrational features of TP are analysed in various solvents (carbon tetrachloride, chloroform, methanol, dimethyl sulfoxide, and water) by employing Polarized Continuum (PCM) Model.

2. Experimental

1,2,4-triazolo-[1,5-a]pyrimidine (TP) was purchased from Aldrich and used without further purification. The infrared spectrum is recorded between 3500 and 550 cm^{-1} on a Bruker Vertex 80 FT-IR spectrometer, and the sample of the free ligand was examined by Pike MIRacle ATR apparatus. Far-IR spectrum was recorded between 700 and 40 cm^{-1} on Bruker IFS 66/S system. The Raman spectrum of TP was recorded between 3500 and 50 cm^{-1} on Bruker FRA 106/S spectrometer, using 1064 nm excitation from a Nd:YAG laser. The detector is a liquid nitrogen-cooled Ge detector.

3. Computational

All the calculations were carried out by using Gaussian 03W package [28] on a personal computer. The geometry of TP was optimized, and its vibrational frequencies were calculated in the gas phase and in CCl_4 ($\varepsilon = 2.228$), chloroform ($\varepsilon = 4.9$), methanol ($\varepsilon = 32.63$), DMSO ($\varepsilon = 46.7$), and water ($\varepsilon = 78.3$) at the B3LYP/6–311++G(d,p) level of theory. The effect of solute-solvent interactions on geometries, vibrational frequencies, and dipole moments was modeled using the self-consistent reaction field (SCRF) method within the Tomasi's Polarized Continuum Model (PCM) [29]. Using the gas phase optimized structures as starting points, all the geometries were re-optimized at the B3LYP/6-311++G(d,p) level by employing the PCM model in different solvents. Assignments of the calculated normal modes were made according to the corresponding total energy distributions (TEDs). The TEDs were calculated by using the Parallel Quantum Solutions software [30]. The theoretical Raman intensities were calculated according to the formula

$$I_i^R = C.(\nu_0 - \nu_i)^4.\nu_i^{-1}.[1 - exp(-h\nu_i c/kT)]^{-1}.S_i^R \quad (1)$$

where ν_i is the calculated frequency of normal mode Q_i, S_i^R is the Raman scattering activity of the normal mode Q_i, C is a constant which is equal to 10^{-12} [31]. In this equation h, k, c, and T are Planck and Boltzmann constants, speed of light and temperature in Kelvin, respectively. ν_0 is the excitation frequency of the laser line (in this study we have used $\nu_0 = 9398.5\ cm^{-1}$ which corresponds to the wavelength of 1064 nm of a Nd:YAG laser), and I_i^R is given in arbitrary units. NMR chemical shifts were calculated using the Gauge Independent Atomic Orbital (GIAO) method and presented with respect to the reference compound tetramethylsilane (TMS).

4. Results and discussion

4.1. Molecular structure of TP

1,2,4-Triazolo-[1,5a]-pyrimidine (TP) molecule has 13 atoms, and it consists of a pyrimidine and a triazole ring fused together. The C=N and C=C bands in the triazolopyrimidine ring (TP) reveal a more pronounced double-bond character, due to the π-electron localization [20]. B3LYP/6-311++G(d,p) optimized geometry and atoms numbering of TP are shown in Fig. 1. Geometrical parameters are listed in Supplementary information (Table S1) together with the experimental data taken from literature [19,21,22,32].

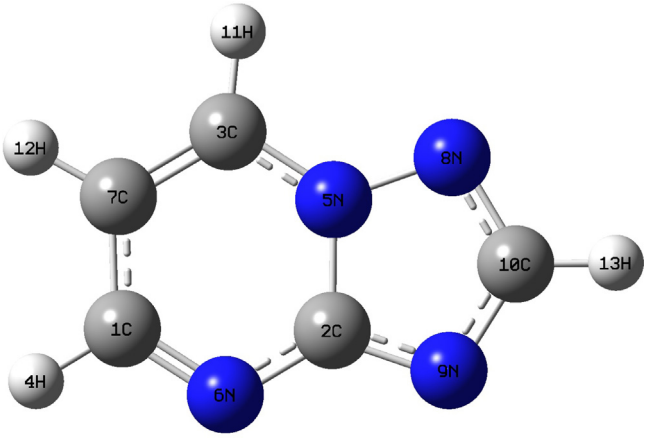

Fig. 1. 1,2,4 triazolo [1,5-a] pyrimidine (TP) molecule and atoms numbering.

The optimized geometry of TP in the ground state corresponds to C_s symmetry group. The data presented in Supplementary information (Table S1) show that B3LYP/6–311++G(d,p) level of calculations have given suitable results which are concordant with published experimental data. Maximum deviation between experiment and theory is 0.035 Å for bond lengths and 3° for bond angles. These deviations may be attributed to the solid-state inter-molecular interactions related to the strong hydrogen bonding and crystal packing effects [33].

C1—N6, C2—N9, C10—N9, C10—N8, C2—N5, and C3—N5 bond lengths are 1.322 Å (calc. 1.317 Å), 1.330 Å (calc. 1.329 Å), 1.352 Å (calc. 1.349 Å), 1.322 Å (calc. 1.334 Å), 1.372 Å (calc. 1.405 Å), and 1.364 Å (calc. 1.355 Å), respectively, which indicate the presence of distinct single and double bonds between nitrogen and carbon atoms, and are in good consistency. The optimized bond angles of N6—C2—N9, C2—N5—N8, C1—N6—C2, and N8—C10—N9 are 130.199°, 110.010°, 116.563°, and 116.932° respectively, which are in good accordance with X-ray data.

The solvent effects on the molecular geometry of TP molecule was investigated with PCM. The gas phase structure was reoptimized at the same level of theory, using the same basis set, and by employing the PCM model.

The mean absolute deviation (MAD) values of calculated bond lengths from experiment are 0.0017, 0.0019, 0.0020, 0.0044 and 0.0017 Å, for the calculated structure in CCl_4, chloroform, methanol, DMSO and water, respectively. For the bond angles, the deviations between theory and experiment are found to be 0.3354° for CCl_4, 0.3224° for chloroform, 0.3102° for methanol, 0.3092° for DMSO, and 0.3117° for water. The differences between the experimental and theoretical results could be attributed to the existence of crystal packing forces in the solid phase which are non-existent in solution.

Analysis of calculation results showed that, on going from gas phase to solvation phase, there were slight changes in the bond lengths. For example, several bond lengths like C1—C7 and C2—N5 were predicted to be longer in the gas phase comparing to those in the solvents whereas C2—N9 and C10—N9 bonds were calculated shorter in the gas phase than those in solvent media.

The N—N and C—H bond lengths increased on going from the gas phase to the solvation phase. Similar type of changes in the values of the bond angles have also been noticed on going from the gas phase to the solvation phase. For example, bond angles like 6N—2C—9N and 2C—5N—8N were decreased with the increased solvent polarity while 5N—3C—11H and 8N—10C—13H increased from gas phase to aqueous solution. The results revealed that the geometrical structures were affected by the solvent effect.

4.2. Vibrational modes

All of the fundamental vibrational frequencies of TP were calculated by using the B3LYP method and 6-311++G(d,p) basis set, and then scaled by 0.9982 [34]. Experimental FTIR and Raman spectra of TP are shown in Fig. 2. The measured and calculated vibrational frequencies, IR intensities and Raman intensities for the TP along with corresponding vibrational assignments and intensities are given in Table 1. There is a good agreement between the experimental and theoretical vibrational frequencies.

Having C_s point group symmetry, TP molecule has 13 atoms and 33 modes of fundamental vibrations which span the irreducible representation as 23A' + 10A". Our calculated frequencies are slightly higher than the observed values for the majority of the normal modes due to the calculations are utilized for harmonic approach.

C—N stretching bands in the pyrimidine ring are predicted at 790 cm^{-1}, 1339 cm^{-1}, 1472 cm^{-1}, and 1657 cm^{-1} (modes 10, 23, 26, and 29). These bands are observed at 800 cm^{-1} (Ra 801 cm^{-1}), 1349 cm^{-1} (Ra 1351 cm^{-1}), 1454 cm^{-1} (Ra 1459 cm^{-1}), and 1620 cm^{-1} (Ra 1622 cm^{-1}) in the experimental spectra. For the triazolo ring C—N stretching bands are predicted at 1192 cm^{-1}, 1237 cm^{-1}, and 1385 cm^{-1} (modes 19, 21, and 24). They are observed at 1186 cm^{-1} (Ra 1199 cm^{-1}), 1229 cm^{-1} (Ra not observed), and 1391 cm^{-1} (Ra 1393 cm^{-1}) in the experimental spectra.

The two most characteristic bands of TP and its derivatives are reported as ν_{tp} (1612–1637 cm^{-1}) and ν_{py} (1515–1550 cm^{-1}) by Szłyk et al. [20–22]. In their work, these bands have been defined as the whole triazolopyrimidine ring skeletal vibration and the pyrimidine ring skeletal vibration, respectively. On the other hand, we have observed ν_{py} at 1620 cm^{-1} (Ra 1622 cm^{-1}, calc. 1657 cm^{-1}) with very strong intensity and assigned it as a mixed mode of C—N and C—C stretching vibrations in the pyrimidine ring. In addition, we also have observed ν_{tp} at 1532 cm^{-1} (Ra not observed, calc. 1562 cm^{-1}) with very strong intensity. According to the results of TED (total energy distribution) analysis, although this mode is mainly contributed by C—N stretching vibrations in the pyrimidine ring it is also partly contributed by the stretchings in triazolo ring. This suggests that this mode is the whole triazolopyrimidine ring skeletal vibration.

Vibrational spectroscopy is a very sensitive tool which is commonly used to probe the solute–solvent interactions [35]. To clarify the vibrational frequencies, it is essential to examine the geometry of any compound since small changes in geometry can potentially cause substantial changes in vibrational frequencies [36]. Our results also reveal that the dielectric medium has significant effect on vibrational frequencies. Changes computed in solvation phase are given in Table 1 on going from the gas phase to different dielectric media. All optimizations have been carried out at B3LYP/6-311++G(d,p) level in the gas phase and in CCl_4, chloroform, methanol, DMSO and water solvents. Gas phase geometry has been used as starting structure in the further calculations.

Frequency deviations are predicted while passing from gas phase to solvation phase. On going from gas phase to polar solvent (water), it has been seen that the vibrational modes 9, 14, 15, and 16 show upshift of 8, 6, 14, and 22 cm^{-1}, respectively. In non-polar solvent (CCl_4), the modes 9, 14, 15, and 16 show upshift of 5, 3, 5 and 9 cm^{-1}, respectively. Besides, the modes 1, 2, 3, 4, 5, 6, 7, 8, 12, and 13 remain almost unaltered. A relatively larger shift in the vibrational bands of TP in DMSO results from the relatively large dipole moment of DMSO. A strong dipole–dipole interaction between TP – DMSO results in a larger frequency shift in the vibrational bands of TP.

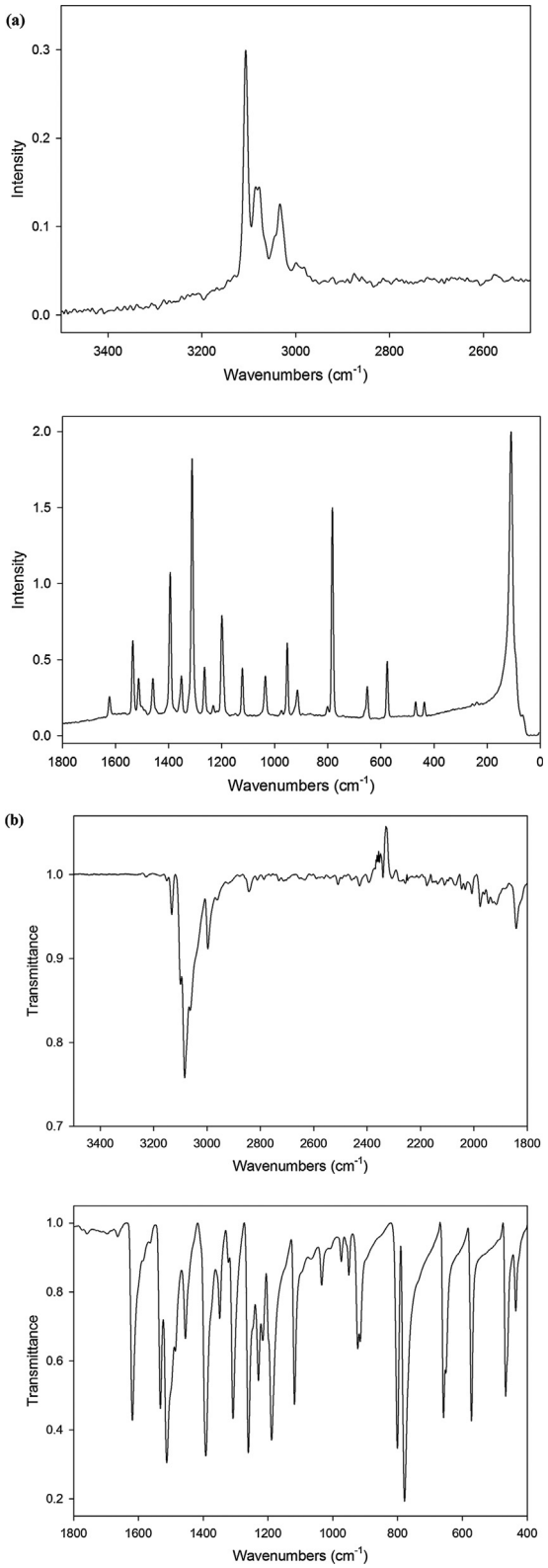

Fig. 2. Experimental (a) Raman (b) Mid-IR spectra of 1,2,4 triazolo[1,5-a] pyrimidine in solid state.

While passing from lower to higher dielectric, the dipole moment increases and there are very significant shifts in vibrational frequencies due to dielectric medium. The C—H bond lengths increased on going from the gas phase to the solvation phase. Hence, the C—H stretching frequencies in pyrimidine ring

Table 1
Experimental and calculated vibrational frequencies (scaled and unscaled) (in cm^{-1}), calculated vibrational frequency shifts ($\Delta\upsilon$) (in cm^{-1}) of TP in different solvents and TEDs obtained for the gas phase.

		B3LYP/6-311G++(d,p)				Experimental		ε = 1	ε = 2.228	ε = 4.9	ε = 32.63	ε = 78.3	
Mode	Sym.	Calc.	Sca.	I inf.	I Ra.	IR	Ra	$\Delta\upsilon$[a]	$\Delta\upsilon$	$\Delta\upsilon$	$\Delta\upsilon$	$\Delta\upsilon$	TED (≥5%) (B3LYP)
1	A"	214	214	2.0	0	211vw	110vs	0	0	2	1	3	$\Gamma_{CNCN}(37) + \Gamma_{CNNC}(20) + \Gamma_{CNCN}(14)$ (py) + $\Gamma_{NNCC}(11)$
2	A"	247	247	0.0	1	237m	–	0	1	4	2	2	$\Gamma_{NNCN}(15) + \Gamma_{CNCN}(15) + \Gamma_{CNCC}(12)$ (py) + Γ_{CNCN} (11) (py) + $\Gamma_{NNCC}(12) + \Gamma_{CCCN}(5)$ (py)
3	A"	425	424	0.6	9	435m	436w	1	1	2	2	4	$\Gamma_{CNCC}(23)$ (py) + $\Gamma_{CCCN}(15)$ (py) + $\Gamma_{CNCN}(10) + \Gamma_{CCCH}(11)$ (py) + $\Gamma_{NNCN}(6)$ (py) + $\Gamma_{CNCN}(9)$ (py) + $\Gamma_{CNCH}(8) + \Gamma_{CNNC}(6)$
4	A'	472	471	6.6	8	468vs	576s	- 1	−2	−2	−2	0	$\delta_{NNC}(26) + \delta_{NCN}(18) + \delta_{CNC}(13)$ (py) + $\delta_{NCN}(9)$ (py)
5	A"	578	577	3.8	0	572vs	–	0	0	1	0	0	$\Gamma_{CCCN}(28)$ (py) + $\Gamma_{CNCC}(11)$ (py) + $\Gamma_{CCCH}(9)$ (py) + $\Gamma_{CNCN}(9) + \Gamma_{NNCN}(8)$ (tr) + $\Gamma_{NNCC}(6) + \Gamma_{CNNC}(5)$ (tr)
6	A'	582	581	3.0	34	651m	**651m**	0	−1	−1	−1	1	$\delta_{CNC}(20)$(py) + $\delta_{NCC}(18)$(py) + $\delta_{NCN}(8)$(py) + $\nu_{NC}(7)$ (tr) + $\delta_{NCN}(7) + \delta_{CCC}(5)$(py) + $\delta_{CCH}(5)$(py)
7	A'	660	659	1.2	25	659vs	–	0	−1	−1	−1	0	$\Gamma_{NCNN}(29)$(tr) + $\Gamma_{NCNC}(24)$(tr) + $\Gamma_{CNNC}(12)$(tr) + $\Gamma_{HCNN}(7)$(tr) + $\Gamma_{CNCN}(5)$(tr) + $\Gamma_{HCNC}(5)$(tr)
8	A"	664	663	7.8	5	670vw	–	0	0	1	1	0	$\nu_{NC}(26)$ (py) + $\delta_{NCN}(13)$(tr) + $\delta_{NNC}(11)$(tr) + $\delta_{CCC}(8)$(py) + $\delta_{CNC}(6)$ (py) + $\delta_{NCN}(5)$ (py) + $\delta_{NCC}(7)$(py) + $\delta_{CNC}(6)$(tr) + $\delta_{HCC}(5)$ (py)
9	A"	775	774	18.7	0	778vs	**782vs**	5	7	11	10	8	$\Gamma_{CNCN}(25)$(py) + $\Gamma_{CNCC}(15)$(py) + $\Gamma_{NNCN}(12)$(tr) + $\Gamma_{CNCN}(11)$ (tr) + $\Gamma_{CCCN}(5)$(py) + $\Gamma_{NCNC}(5)$(tr)
10	A"	791	790	45.1	1	800vs	**801w**	3	4	5	5	6	$\Gamma_{HCCN}(51)$(py) + $\nu_{NC}(35)$(py) + $\nu_{NC}(19) + \nu_{NN}(12)$(tr) + $\nu_{CC}(6)$ (py) + $\delta_{NCC}(5)$(py)
11	A'	794	793	1.3	90	–	–	1	2	5	4	5	$\Gamma_{CNCH}(14)$(py) + $\Gamma_{CCCH}(13)$(py) + $\Gamma_{NNCH}(13)$
12	A'	920	918	0.0	37	915w	**914m**	0	0	0	0	3	$\delta_{CCC}(13)$(py) + $\delta_{NCC}(13)$(py) + $\nu_{NN}(12)$(tr) + $\nu_{NC}(11) + \nu_{NC}(9)$ (tr) + $\delta_{CNC}(8)$(py) + $\delta_{CNC}(5)$(tr) + $\delta_{NCH}(5)$(py)
13	A"	927	925	9.1	0	922m	–	0	1	1	1	2	$\Gamma_{HCNC}(44)$(tr) + $\Gamma_{HCNN}(43)$(tr)
14	A'	950	948	0.8	8	950vw	**953s**	3	6	8	8	6	$\nu_{NC}(19) + \delta_{NCN}(19)$(tr) + $\delta_{CNN}(15)$(tr) + $\nu_{CC}(6)$(py) + $\delta_{HCN}(7)$(tr) + $\nu_{CN}(6)$(tr) + $\delta_{CNC}(6)$(tr) +
15	A"	953	951	0.2	0	**–**	–	5	8	10	10	14	$\Gamma_{HCCH}(54)$(py) + $\Gamma_{CNCH}(19)$ (py) + $\Gamma_{CCCH}(15)$(py)
16	A"	962	960	1.0	1	973vw	–	9	15	20	20	22	$\Gamma_{HCCH}(36)$(py) + $\Gamma_{CCCH}(24)$(py) + $\Gamma_{CNCH}(20)$ (py) + $\Gamma_{NNCH}(12) + \Gamma_{HCCN}(6)$(py)
17	A'	1049	1047	2.2	31	1118s	**1035m**	2	4	5	5	7	$\nu_{CC}(55)$ (py) + $\delta_{HCC}(13)$ (py) + $\delta_{HCC}(6)$ (py)
18	A'	1133	1131	4.4	4,1	–	**1122m**	−2	−4	−6	−6	3	$\delta_{HCC}(34)$(py) + $\delta_{CCH}(20)$(py) + $\nu_{CC}(12)$(py) + $\nu_{NN}(7)$(tr) + $\delta_{NCH}(6)$(py)
19	A'	1194	1192	48.9	43	1186vs	**1199s**	4	5	4	4	11	$\nu_{CN}(28)$(tr) + $\delta_{HCN}(20)$(tr) + $\nu_{NC}(8) + \nu_{NC}(7)$(py) + $\nu_{CC}(8)$ (py) + $\nu_{NN}(6)$(tr) + $\delta_{NCN}(5) + \delta_{CNC}(6)$(tr)
20	A'	1211	1209	23.5	24	1216w	**1234vw**	−2	−2	−1	−1	1	$\delta_{HCN}(28)$(tr) + $\nu_{NN}(17)$(tr) + $\nu_{CC}(10)$(py) + $\delta_{HCC}(7)$ (py) + $\nu_{CN}(6)$(tr)
21	A'	1239	1237	17.9	10	1229s	–	1	2	4	4	8	$\nu_{CN}(52)$(tr) + $\nu_{NC}(14)$(py) + $\delta_{HCN}(5)$(py) + $\delta_{HCC}(6)$(py) + $\delta_{NCN}(6) + \delta_{NCH}(6)$
22	A'	1299	1297	44.4	29	1308s	**1311vs**	−4	−8	−10	−11	−5	$\nu_{CN}(46)$(tr) + $\nu_{NN}(10)$(tr) + $\delta_{NCN}(10)$(tr) + $\delta_{HCN}(10)$(tr) + $\nu_{NC}(5)$ (py)
23	A'	1341	1339	35.3	43	1349m	**1351w**	−3	−6	−8	−9	−2	$\nu_{NC}(21)$(py) + $_{CN}(13)$(tr) + $\delta_{HCC}(13)$(py) + $\delta_{CCH}(8)$ (py) + $\nu\nu_{CC}(5)$(py) + $\nu_{NC}(5) + \nu_{NN}(6)$(tr) + $\delta_{NCN}(5)$(tr) + $\delta_{NCH}(6)$(py) + $\delta_{HCN}(5)$(tr)
24	A'	1387	1385	28.1	13	1391vs	**1393s**	−7	−11	−15	−16	−5	$\nu_{NC}(30)$(tr) + $\delta_{HCN}(29)$(py) + $\delta_{HCC}(16)$(py) + $\nu_{NC}(6)$(py)
25	A'	1430	1427	23.1	78	–	–	−4	−7	−11	−11	−3	$\nu_{NC}(32)$(py) + $\delta_{NCH}(14)$(py) + $\delta_{CCH}(11)$(py) + $\nu_{CN}(6)$ (tr) + $\delta_{HCC}(7)$(py) + $\delta_{HCN}(6)$(tr)
26	A'	1475	1472	17.0	13	1454m	**1459m**	−3	−4	−5	−6	2	$\nu_{NC}(21)$(py) + $\nu_{CN}(16)$(tr) + $\delta_{HCN}(4)$(py) + $\delta_{HCC}(6)$(py) + $\delta_{CNN}(7)$(tr)
27	A'	1547	1544	104.3	14	1512vs	**1534s**	−3	−6	−9	−10	−3	$\nu_{CC}(34)$(py) + $\delta_{HCC}(16)$(py) + $\nu_{NC}(13)$(py) + $\nu_{NC}(5)$
28	A'	1565	1562	21.3	17	1532vs	–	−3	−3	−3	−3	1	$\nu_{NC}(26)$(py) + $\nu_{NC}(22)$(tr) + $\delta_{HCC}(11)$(py) + $\delta_{HCN}(7)$(py) + $\nu_{CC}(7)$ (py)
29	A'	1660	1657	92.2	7	1620vs	**1622vw**	−4	−7	−9	−10	−6	$\nu_{NC}(36)$(py) + $\nu_{CC}(25)$(py) + $\nu_{NC}(5)$(tr) + + $\delta_{NCH}(6)$(py)
30	A'	3157	3151	10.9	55	2997w	**3085sh**	−19	−35	−54	−55	19	$\nu_{HC}(98)$(py)
31	A'	3214	3208	0.4	34	3083m	**3106m**	−30	−57	−86	−88	12	$\nu_{HC}(99)$(py)
32	A'	3228	3222	0.7	64	3132vw	–	−31	−55	−80	−82	11	$\nu_{HC}(98)$(py)
33	A'	3246	3240	2.3	53	–	–	−30	−55	−81	−83	0	$\nu_{HC}(99)$(tr)

[a] $\Delta\nu = \nu_{sol}^{scal} - \nu_{gas}^{scal}$.
I inf.: infrared intensity, I Ra.: relative Raman intensity (arbitrary units).
sh: shoulder, vw: very weak, w: weak, m: medium, s: strong, vs: very strong, py: pyrimidin, tr: triazole, υ: stretch, δ: in-plane bending, Γ: out-of-plane bending.

should decrease. On the other hand, C—H bond lengths have been decreased and thus the C—H frequencies should have been increased accordingly for the aqueous solution. It is clearly seen from Table 1 that these requirements are fulfilled for TP. While mode 33 arises from triazolo ring is a C—H vibration which shifts by 30 upto 83 cm^{-1} when going from gas phase to solution, no shifting is predicted for aqueous solution. Pyrimidine C—H modes (30, 31, and 32) have also showed large frequency shifts from 19 up

to 88 cm^{-1}, though frequency shifts in aqueous solution are relatively small. These frequency shifts are explained in terms of increased positive character of carbons in the pyrimidine ring.

The pyrimidine ring torsion (H—C—C—H and C—C—C—H) vibrations are assigned to 951 and 960 cm^{-1} in the gas phase. These bands were shifted upward by 5 to 22 cm^{-1} in solution. On the other hand, N—C—N in-plane bending vibration computed as modes 4, 6, and 8, remain almost unaltered. In addition, the modes contributed by N—N stretching vibrations in the triazolo ring (modes 10, 20, and 22) have shown a maximal shift of 11 cm^{-1}. However, mode 12 which includes an N—N stretching vibration of the triazolo ring remained unchanged. A similar behavior occured for the C—C stretching modes of 17 and 27, and an upshift of 7 cm^{-1} and downshift of 10 cm^{-1} were observed, respectively.

According to these results, from lower to higher dielectric medium, the dipole moment increases and there are significant shifts in vibrational frequencies due to dielectric medium.

4.3. Atomic charges

The atomic charges in TP molecule in the gas and solvation phases computed by Natural Population Analysis (NPA) with B3LYP/6-311++G(d,p) level are demonstrated in Supplementary information (Table S2). As determined in our study, atomic charge distribution over TP molecule varies for any atom by changing solvent polarity [37]. For example, the largest negative charge (−0.507 e) is localized on N9 atom of the triazolo ring of TP which is similar to the previous theoretical approaches [38]. An increase of negative charge was also observed on N6 atom in the pyrimidine ring and N9 atom in the triazolo ring with increasing polarity. While the negative charges on N6, N8, N9 atoms regularly increased, a slight variation was observed on N5 (from −0.223 e to −0.214 e) and C7 (from −0.298 e to −0.292 e). Hence, we have concluded that the negative charge led to the redistrubition of electron density. On the other hand, the positive charges increase while passing from gas phase to solvation phase. Although the calculated distribution of positive charges on all hydrogen atoms were regularly increasing with the increasing dielectric constant (ε) of the medium, positive charge on C10 atom remained stable. The maximum atomic charge was observed on C2 atom comparing to other atoms in polar and non-polar solvents. C2 atom accommodates higher positive charge due to the strong negative charges observed within the ring. Results both indicate that the charge distributions are sensitive to dielectric media, and the coordination ability of C and N atoms would be changed in different solvents which might be helpful when one wants to use title compound to construct interesting metal complexes with different coordination geometries [39].

4.4. Frontier molecular orbitals

The highest occupied molecular orbital (HOMO) and lowest unoccupied molecular orbital (LUMO) are the main orbitals taking part in chemical stability. The HOMO represents the ability to donate an electron and LUMO represents the ability to accept an electron [40]. Molecular orbitals and their properties are very informative for physicists and chemists. Frontier molecular orbitals are also used to predict the most reactive position In π-electron systems and also they explain several types of reactions in conjugated systems [41]. Fig. 3 shows that the HOMO of TP has bonding nature between the atoms 8N—10C, 3C—5N—2C—9N, 7C—1C—6N, whereas it has anti-bonding nature between the atoms 8N—5N, 10C—9N, 2C—6N, 3C—7C. On the other hand, LUMO exhibits anti-bonding nature for 1C—7C, 9N—2C—5N, and bonding nature between 5N—3C, 3C—7C, 10C—9N, 2C—6N, 6N—1C.

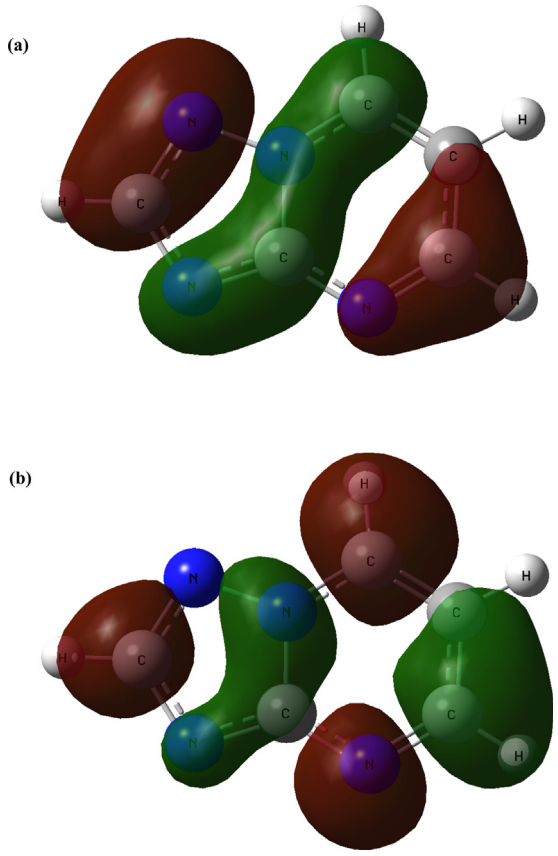

Fig. 3. The isosurfaces (green: positive, red: negative) of (a) HOMO and (b) LUMO of TP in the gas phase.

Quantum chemical descriptors have been widely used for QSAR (quantitative structure-activity relationship) studies on the biological activity of compounds. The atomic partial charges, HOMO–LUMO energies, frontier orbital densities, and other quantum chemically calculated descriptors have been shown to correlate well with various biological activities [42]. Eigenvalues of HOMO, LUMO, and the gap between them reflect the chemical activity of the molecule. Besides, the HOMO and the LUMO are responsible for the charge transfer [42]. Recently, the energy gap between HOMO and LUMO has been used to prove the bioactivity from intramolecular charge transfer (ICT) [41,43,44].

Our computational results indicate that when in solvation phase, electron density distributions are almost the same of gas phase electronic density. Hence, the electrostatic field contour maps of HOMO and LUMO of TP in solvation phase are not presented in here. Besides, it has been seen that the LUMO−HOMO energy gap of TP is marginally affected by the presence of solvent. The energy gap values are computed as 5.240, 5.216, 5.246, 5.248, and 5.268 eV for CCl_4, chloroform, methanol, DMSO, and water respectively. For the gas phase, the HOMO-LUMO energy gap of TP is calculated as 5.138 eV.

4.5. Solvation energy, solvation free energy, and dipol moment

Solvent effects improve the charge delocalization in the molecules, therefore the dipole moment of the system become induced and raised in magnitude. Hence, solvent energies show correlation with the dielectric constants or dipole moments. Ground-state dipole moment is an important factor in measuring

solvent effects, a large ground-state dipole moment gives rise to a strong solvent polarity effect [45].

Table 2 includes the calculation results for solvation energies (ΔE_{solv}), solvation free energies (ΔG_{solv}), and dipole moments of TP in the gas phase, and in non-polar and polar solvents predicted at B3LYP/6-311++G(d,p) level of theory. Dipole moments affect intermolecular interactions in substances. Due to the additional dipole moment induced by the solvents, a polar molecule will have a larger dipole moment in a polar solvent than in the gaseous phase, which in turn will increase the stability of the molecular system [46]. The dipole moment is expected to be larger in solution than the corresponding dipole moment in the gas phase. Calculated dipole moments increase while passing from gas phase to solvation phase, mainly due to major charge redistribution in the molecule, and also by changes in the distances between the charge separations [47].

As seen from Table 2, the dipole moment increases in solvation phase and is sensitive to the polarity of the solvent medium. Besides, the increase predicted in the dipole moment is more apparent for polar solvent. The dipole moment of TP molecule was found to be 4.32 Debye in the gas phase and 5.15, 5.76, 6.36, 6.40 and 6.08 Debye in chloroform, CCl_4, methanol, DMSO and water, respectively.

The dipole moment has some relationship with the solvation energy. The interaction between the solute molecules and solvent (polar and non-polar) molecules, namely solvation energy, is stronger with large dipole moment than the one with small dipole moment [47]. Solvation energies depend only on the molecular structure and electronic distribution, and are usually not strongly basis set or model dependent [48]. Since the larger dipole moment causes larger solvation energy, this results in better stabilization of the molecular system when in solvation phase. Moreover, the solvent with larger dielectric constant results in larger stabilization energy for the polar species. In our study, the order of solvation energies for TP is predicted as follows: DMSO < methanol < chloroform < water < CCl_4.

The solvation free energy, ΔG_{solv}, is the work needed to transfer molecule from gas phase into solution [49]. It plays a significant role in the understanding of the chemical behavior of molecules in condensed phase. Since it represents the desolvation cost of a ligand binding to a receptor, solvation free energy is considered as an important molecular characteristic in drug discovery studies. Most of the recent developments in the estimation of solvation free energy require the use of molecular mechanics and dynamics calculations. Calculated ΔG_{solv} of TP are listed in Table 2. The ΔG_{solv} value is expected to increase with solvent polarity, and thus, solvation of TP increases with the polarity of the solvent. The data on ΔG_{solv} values in Table 2 shows that the value of ΔG_{DMSO} is more negative than that of methanol, water, chloroform, and CCl_4 which means that the solvation of TP in DMSO is better than in other mentioned solvents.

4.6. Nuclear magnetic resonance

Experimental ^{1}H, ^{13}C, and ^{15}N NMR spectra of TP ligands were reported by the previous studies [21,22,50,51]. In our study, the NMR chemical shifts were obtained theoretically using the Gauge Independent Atomic Orbital (GIAO) method at the B3LYP/6–311++G(d,p) level in the Gaussian 03W software package. Tetramethylsilane (TMS) was accepted as internal reference, and the solvent employed was DMSO. The data were reported in ppm as shifts with respect to TMS. Note that theoretical ^{13}C NMR shifts were scaled according to the scaling equation $d_{scal} = 0.95 d_{calc} + 0.30$ before comparing with experimental data [52]. Theoretical chemical shifts of all tautomers and the previously published experimental data are given in Table 3. Calculated chemical shifts correlate well with the experimental data. The linear correlations between theoretical and experimental data are determined. The squared correlation factors (R^2) are 0.999 when our results are compared with the experimental results published before. We do not report any correlation factors for ^{1}H NMR for a reason. A good correlation for proton shifts was not expected, since the protons are located on the periphery of the molecule and are supposed to be more susceptible to solute-solvent effects [53].

Table 2
Solvation energies ([a]ΔE_s), solvation free energies ([b]ΔG_s), and dipol moments μ (in Debye) of TP in the gas phase and in different solvents.

	$\varepsilon = 1$	$\varepsilon = 2.228$	$\varepsilon = 4.9$	$\varepsilon = 32.63$	$\varepsilon = 46.7$	$\varepsilon = 78.3$
[a]ΔE_s	0	−21.0040	−35.4443	−50.4096	−51.1972	−35.1851
[b]ΔG_s	0	−21.6551	−37.2295	−52.5336	−53.4341	−34.1604
μ	4.3284	5.1506	5.7557	6.3646	6.4007	6.0821

[a]$\Delta E_s = E_{solution} - E_{gas}$ (in kJ/mol).
[b]$\Delta G_s = G_{solv} - G_{gas}$ (in kJ/mol).

5. Conclusion

We have conducted a combined experimental and theoretical investigation on the spectroscopic, structural, and electronic properties of 1,2,4-triazolo-[1,5-a]pyrimidine (TP). The gas phase geometry and vibrational features of the title ligand were computed and compared with the experimental results. A complete assignment of vibrational frequencies was proposed by using total energy distribution analysis. Solvent effects on the spectroscopic, structural and electronic properties of TP were also analysed computationally in chloroform, carbon tetrachloride (CCl_4), methanol, dimethyl sulfoxide (DMSO) and water. It has been seen that there is a relationship between the dielectricity of solvent media and the investigated features of TP. Solvation energy and solvation free energy of TP are decreased while the dielectric constant of the media increased. Hence, the stability of TP is increased. Introducing the solvation model caused only small variations on the geometrical parameters of TP. On the other hand, vibrational frequencies are affected by the change of medium. Torsional vibrations in the triazolopyrimidine skeleton are significantly affected. C−H bands of the title compound are also strongly perturbed. The dipole moment of TP is correlated with the dielectric constants of the media, and due to larger dipole moment the TP structure becomes more stable in solution. Calculated natural atomic charges on TP show that the nitrogen atoms of the triazolopyrimidine skeleton are rich in negative charge. Charge distribution on TP skeleton is affected by the solvent in small extent, though the charges on 6N, 8N, and 9N are found to be sensitive to dielectric medium. On the other hand, the frontier electron distribution over TP and the LUMO−HOMO energy gap is almost not affected from the presence of a dielectric medium.

Table 3
Theoretical [a] and experimental chemical shifts (in ppm) of 1,2,4-triazolo[1,5-a] pyrimidine.

Atoms [b]	Exp. [c]	Exp. [d]	Exp. [e]	Exp. [f]	TP
1C	156.7	156.1	156.0	155.5	155.3
2C	154.1	156.0	155.1	154.6	155.7
3C	138.7	138.0	138.1	137.4	137.7
7C	109.9	111.6	111.3	110.9	111.4
10C	154.7	156.7	156.3	155.8	156.7
4H	–	–	8.91	–	9.40
11H	–	–	9.43	–	9.60
12H	–	7.47	7.38	–	7.80
13H	–	8.72	8.69	–	9.00

[a] Solvent is DMSO.
[b] Atom numberings as given in Fig. 1.
[c,d,e,f] See Refs. [21,22,50,51].

Acknowledgements

The authors would like to thank the editor and the reviewers for their comments that help improve the manuscript.

Appendix A. Supplementary data

Supplementary data associated with this article can be found, in the online version, at http://dx.doi.org/10.1016/j.vibspec.2017.08.011.

References

[1] G. Fischer, Z. Chem. 30 (1990) 305–315.
[2] G. Fischer, Adv. Heterocycl. Chem. 57 (1993) 81–86.
[3] E.S.H. Elashry, N. Rashed, Adv. Heterocycl. Chem. 72 (1999) 127–224.
[4] W.A. Kleschick, M.J. Costales, J.E. Dunbar, R.W. Meikle, W.T. Monte, N.R. Pearson, S.W. Snider, A.P. Vinogradoff, Pestic. Sci. 29 (1990) 341–355.
[5] R.B. Shankar, R.G. Pews, J. Heterocycl. Chem. 30 (1993) 169–172.
[6] G.F. Yang, H.Z. Yang, Heteroat. Chem. 11 (2000) 313–316.
[7] E. Tenor, R. Ludwig, Pharmazie 26 (1971) 534–539.
[8] K. Jelich, W. Kraemer, H.J. Santel, R.R. Schmidt, H. Strang, Ger. offen. DE 3640, 155, Chem. Abs. 109 (1988) 93057f.
[9] D. Duerr, Eur. Pat. Appl. EP 434624, Chem. Abs. 115 (1991) 159165x.
[10] T. Novinson, R.H. Springer, D.E. O'Brien, M.B. Scholten, J.P. Miller, R.K. Robins, J. Med. Chem. 25 (1982) 420–4426.
[11] J.Z. Deng, D.R. McMasters, P.M.A. Rabbat, P.D. Williams, C.A. Coburn, Y. Yan, L.C. Kuo, S.D. Lewis, B.J. Lucas, J.A. Krueger, B. Strulovici, J.P. Vacca, T.A. Lylea, C.S. Burgey, Bioorg. Med. Chem. Lett. 15 (2005) 4411–4416.
[12] C.B. Vu, P. Shields, B. Peng, G. Kumaravel, X.W. Jin, D. Phadke, J. Wang, T. Engber, E. Ayyub, R.C. Petter, Bioorg. Med. Chem. Lett. 14 (2004) 4435–4438.
[13] P.G. Baraldi, B. Cacciari, R. Romagnoli, G. Spalluto, S. Moro, K.N. Klotz, E. Leung, K. Varani, S. Gessi, S. Merighi, P.A. Borea, J. Med. Chem. 43 (2000) 4768–4780.
[14] T. Okamura, Y. Kurogi, K. Hashimoto, K. Nishikawa, Y. Nagao, Bioorg. Med. Chem. Lett. 14 (2004) 2443–2446.
[15] J.F. Bower, A. Cansfield, A. Jordan, M. Parratt, L. Walmsley, D. Willianson, WO 2004108136. 2004, Chem. Abstr. 141 (2005) P56337h.
[16] M.R. Schmitt, D.R. Kirsch, J.E. Harris, C.F. Beyer, K.J. Pees, P. Carter, W. Pfrengle, G. Albert, WO 0202563. 2002, Chem. Abstr. 136 (2002) P96032n.
[17] N. Zhang, S. Ayral-Kaloustian, T. Nguyen, J. Afragola, R. Hernandez, J.J. Lucas, Med. Chem. 50 (2007) 319–327.
[18] J.M. Salas, M.A. Romero, M.P. Sánchez, M. Quirós, Coord. Chem. Rev. 193–195 (1999) 1119–1142.
[19] E. Szłyk, I. Lakomska, A. Surdykowwski, T. Glowiak, L. Pazderski, J. Sitkowski, L. Kozerski, Inorg. Chem. Acta 333 (2002) 93–99.
[20] E. Szłyk, A. Grodzicki, L. Pazderski, E. Bednarek, B. Kamieński, Polyhedron 19 (2000) 965–969.
[21] E. Szłyk, L. Pazderski, I. Lakomska, A. Surdykowski, T. Glowiak, J. Sitkowski, L. Kozerski, Polyhedron 21 (2002) 343–348.
[22] E. Szłyk, A. Grodzicki, L. Pazderski, A. Wojtczak, J. Chatłas, G. Wrzeszcz, J. Sitkowski, B. Kamieński, J. Chem. Soc. Dalton Trans. 6 (2000) 867–872.
[23] E. Szłyk, L. Pazderski, I. Łakomska, L. Kozerski, J. Sitkowski, Magn. Reson. Chem. 40 (2002) 529–532.
[24] H. Wang, W. Xu, Y. Dai, B. Zhang, Q. Wu, D. Wang, M. Zhang, M. Tian, H. Wu, J. Heterocycl. Chem. 44 (2007) 993–997.
[25] K. Dharmalingam, K. Ramachandran, P. Sivagurunathan, J. Zhejiang Univ. Sci. A 7 (2006) 1928–1931.
[26] O. Dopfer, M. Fujii, Chem. Rev. 116 (2016) 5432–5463.
[27] Ş. Yurdakul, S. Badoğlu, L. Özkurt, Spectrochim. Acta A 162 (2016) 48–60.
[28] M.J. Frisch, G.W. Trucks, H.B. Schlegel, G.E. Scuseria, M.A. Robb, J.R. Cheeseman, J.A. Montgomery, Jr. T. Vreven, K.N. Kudin, J.C. Burant, J.M. Millam, S.S. Iyengar, J. Tomasi, V. Barone, B. Mennucci, M. Cossi, G. Scalmani, N. Rega, G.A. Petersson, H. Nakatsuji, M. Hada, M. Ehara, K. Toyota, R. Fukuda, J. Hasegawa, M. Ishida, T. Nakajima, Y. Honda, O. Kitao, H. Nakai, M. Klene, X. Li, J.E. Knox, H.P. Hratchian, J.B. Cross, V. Bakken, C. Adamo, J. Jaramillo, R. Gomperts, R.E. Stratmann, O. Yazyev, A.J. Austin, R. Cammi, C. Pomelli, J.W. Ochterski, P.Y. Ayala, K. Morokuma, G.A. Voth, P. Salvador, J.J. Dannenberg, V.G. Zakrzewski, S. Dapprich, A.D. Daniels, M.C. Strain, O. Farkas, D.K. Malick, A.D. Rabuck, K. Raghavachari, J.B. Foresman, J.V. Ortiz, Q. Cui, A.G. Baboul, S. Clifford, J. Cioslowski, B.B. Stefanov, G. Liu, A. Liashenko, P. Piskorz, I. Komaromi, R.L. Martin, D.J. Fox, T. Keith, M.A. Al-Laham, C.Y. Peng, A. Nanayakkara, M. Challacombe, P.M.W. Gill, B. Johnson, W. Chen, M.W. Wong, C. Gonzalez, J.A. Pople, Gaussian 03 Revision C.02, Gaussian Inc., Wallingford, CT, 2004.
[29] S. Miertuš, E. Scrocco, J. Tomasi, Chem. Phys. 55 (1981) 117–129.
[30] P. Pulay, J. Baker, K. Wolinski, SQM ver 2.0, Parallel Quantum Solutions, Fayetteville AR 72703, USA, 2007.
[31] D. Michalska, R. Wysokiński, Chem. Phys. Lett. 403 (2005) 211–217.
[32] S. Orihuela, P. Sànchez, M. Quirós, J. Molina, R. Faure, J. Mol. Struct. 415 (1997) 285–292.
[33] M.K. Rofouei, N. Sohrabi, M. Shamsipur, E. Fereyduni, S. Ayyappan, N. Sundaraganesan, Spectrochim. Acta A 76 (2010) 182–190.
[34] H. Watanabe, N. Hayazawa, Y. Inouye, S. Kawata, J. Phys. Chem. B 109 (2005) 5012–5020.
[35] D.K. Singh, S.K. Srivastava, A.K. Ojha, B.P. Asthana, J. Mol. Struct. 892 (2008) 384–391.
[36] E. Güneş, C. Parlak, Spectrochim. Acta A 82 (2011) 504–512.
[37] T. Polat, Ş. Yurdakul, J. Mol. Struct. 1001 (2011) 16–22.
[38] J.W. Wiench, L. Stefaniak, G.A. Webb, J. Mol. Struct. 605 (2002) 33–39.
[39] T. Karakurt, M. Dinçer, A. Çukurovalı, I. Yılmaz, J. Mol. Struct. 991 (2011) 186–201.
[40] S. Subashchandrabose, A.R. Krishnan, H. Saleem, V. Thanikachalam, G. Manikandan, Y. Erdoğdu, J. Mol. Struct. 981 (2010) 59–70.
[41] L. Padmaja, M. Amalanathan, C. Ravikumar, I. Hubert Joe, Spectrochim. Acta A 74 (2009) 349–356.
[42] M. Karelson, Molecular Descriptors in QSAR/QSPR, Wiley, New York, 2000.
[43] L. Padmaja, C. Ravikumar, D. Sajan, I. Hubert Joe, V.S. Jayakumar, G.R. Pettit, O. Faurskov Nielsen, J. Raman Spectrosc. 40 (2009) 419–428.
[44] C. Ravikumar, I. Hubert Joe, V.S. Jayakumar, Chem. Phys. Lett. 460 (2008) 552–558.
[45] Y. Le, H. Ji, J.-F. Chen, Z. Shen, J. Yun, M. Pu, Int. J. Pharm. 370 (2009) 175–180.
[46] Y. Liu, H. Du, G. Wang, X. Gong, L. Wang, H. Xiaon, Int. J. Quantum Chem. 1111 (2011) 1115–1126.
[47] J.-C. Fan, Z.-C. Shang, J. Liang, X.-H. Liu, H. Jin, J. Mol. Struct. Theochem. 939 (2010) 106–111.
[48] K.B. Wiberg, D.J. Rush, J. Am. Chem. Soc. 123 (2001) 2038–2046.
[49] A. Liu, D. Wu, D. Jia, L. Liu, Int. J. Quantum Chem. 110 (2010) 1360–1367.
[50] J.W. Wiench, L. Stefaniak, G.A. Webb, J. Mol. Struct. 605 (2002) 33–39.
[51] A. Salgado, C. Varela, A.M.G. Collazo, P. Pevarello, Magn. Reson. Chem. 48 (2010) 614–622.
[52] A.E. Aliev, D. Courtier-Murias, S. Zhou, J. Mol. Struct. Theochem. 893 (2009) 1–5.
[53] B. Osmialowski, E. Kolehmainen, E. Gawinecki, Magn. Res. Chem. 39 (2001) 334–340.